Facile preparation and photoelectrochemical properties of CdSe/TiO2 NTAs

ARTICLE *in* MATERIALS RESEARCH BULLETIN · MARCH 2012

Impact Factor: 2.29 · DOI: 10.1016/j.materresbull.2011.12.039

Materials Research Bulletin 47 (2012) 580–585

Contents lists available at SciVerse ScienceDirect

Materials Research Bulletin

journal homepage: www.elsevier.com/locate/matresbu

Facile preparation and photoelectrochemical properties of $CdSe/TiO_2$ NTAs

Jiayong Gan [a], Teng Zhai [a], Xihong Lu [a,b], Shilei Xie [a], Yanchao Mao [a], Yexiang Tong [a,*]

[a] Key Laboratory of Environment and Energy Chemistry of Guangdong Higher Education Institutes, MOE Key Laboratory of Bioinorganic and Synthetic Chemistry, School of Chemistry and Chemical Engineering, Institute of Optoelectronic and Functional Composite Materials, Sun Yat-Sen University, Guangzhou 510275, PR China
[b] Department of Chemistry and Biochemistry, University of California, Santa Cruz, CA 95064, United States

ARTICLE INFO

Article history:
Received 23 June 2011
Received in revised form 17 December 2011
Accepted 27 December 2011
Available online 4 January 2012

Keywords:
D. Optical properties
Electronic materials
Nanostructures
Semiconductors

ABSTRACT

In the present work we report the design and synthesis of $CdSe/TiO_2$ nanotube arrays (NTAs) and their implementation as a photoanode for photoelectrochemical (PEC) application. CdSe nanoparticles with well dispersion were decorated on the inner and outer surfaces of 2.5 μm-long TiO_2 nanotubes via electrodeposition. These $CdSe/TiO_2$ NTAs exhibit a significant photocurrent responds under visible light illumination ($\lambda \geq 420$ nm). The results presented in this study display a promising method that the photoelectrochemical performance could be improved via composition, size and crystalline control of $CdSe/TiO_2$ NTAs. And the tubular morphology is also able to facilitate charge transport in nanostructure-based PEC cells. This research demonstrates a new approach, which have great potential applications in fabricating novel heterostructure-photoelectrochemical devices.

1. Introduction

Hydrogen is considered to be a potential candidate for a nonpolluting energy source. Recently, more and more attention is paid to solar energy because of its environmental friendliness and infinite energy resource. Since the innovative report published in 1972 for photoelectrochemical water splitting, considerable efforts have been dedicated to the development of photocatalytic materials or photoelectro-chemical (PEC) cells in order to converse solar energy into hydrogen [1,2]. Solar radiation is ideal to meet the projected demand but requires new initiatives to harvest incident photons with higher efficiency. In these years, research on TiO_2-based photoelectrodes has received significant attention due to their potential application in solar energy conversion [3–7]. In particular, extensive investigations have been devoted to improve the efficiency of TiO_2-based photoelectrodes in PEC cells [8–12].

Although TiO_2 can serve as a stable photoelectrode because of its inherent good corrosion resistance in aqueous solution [13], its large bandgap (3.2 eV) prevents efficient absorption of sunlight in the visible region and results in poor overall energy conversion efficiency. To approach this issue, one method is to use sensitizers to extend the absorption into the visible region, such as dye molecules [14], metal ions-Sn^{4+} [15] and narrow bandgap semiconductor quantum dots (QDs) [16]. Especially, the size-tunable wide bandgap makes QDs particularly attractive as sensitizers [17]. Semiconductor with its tunable band edge offer new opportunities for harvesting light energy in the visible region of the solar spectrum. Ordered assemblies of narrow band gap semiconductor nanostructures are convenient systems to harvest visible light energy. Because they can provide less energy barrier and avoid the particle-to-particle hopping that may occur in the disordered nanostructures when the electrons transfer in them. For example, smaller band gap nanomaterials can effectively extend the photoresponse of TiO_2 into the visible region. Various semiconductors, or even rare earth oxides such as CeO_2, PbS, ZnO, Cu_2O, CdTe, and Bi_2S_3, have been demonstrated as visible light sensitizers for TiO_2-based electrodes [15–26].

Highly ordered, vertically oriented TiO_2 nanotube arrays (NTAs) obtained by anodization have attracted significant interest due to their suitable electrical properties and excellent stability [27]. Compared with the traditional TiO_2 nanocrystal based photoelectrodes, the tube structure can facilitate separation of the photo-excited charges, leading to higher charge collection efficiencies [28]. Nevertheless, the development of facile methods for large-scale fabrication of TiO_2 NTAs and their composite material nanostructures is still in progress.

Various methods have been exploited to synthesize $CdSe/TiO_2$ electrodes with different morphologies. Cao et al. [29] reported an electrospinning method to prepare TiO_2/CdS composite fiber. Moreover, the reported sequential chemical bath deposition method by Sun et al. [21] to synthesize CdS quantum dots into TiO_2 NTs is time-consuming, which is not suitable for practical applications And this method produces both hexagonal and cubic phases of CdS, which is not good for photocatalysis. Electrochemical deposition is a promising method for large-scale fabrication of

* Corresponding author. Tel.: +86 20 84110071; fax: +86 20 84112245.
E-mail addresses: ganjy@student.sysu.edu.cn (J. Gan), chedhx@mail.sysu.edu.cn (Y. Tong).

0025-5408/$ – see front matter © 2012 Elsevier Ltd. All rights reserved.
doi:10.1016/j.materresbull.2011.12.039

nanomaterials owing to its simplicity, template-free, low cost, and environmental friendliness [30,31]. This method offers an easy control over all the reaction factors, as well as gives a better bonding between the semiconductors. This process not only reduces many complicated and time-consuming steps to fabricate the NTAs but also gives better stability to the photocatalyst. Herein, based on a template- and surfactant-free electrochemical deposition method, we report an approach for the synthesis of a hybrid nanotube arrays structure in which CdSe and TiO_2 bind together strongly without linker molecules. This resulting structure may be able to strengthen the photostability of CdSe on TiO_2 NTAs. This approach has obvious advantages due to its simplicity, ease of scale-up, and low costs. Furthermore, the CdSe/TiO_2 hybrid nanostructure is expected to have higher electron injection efficiency and better PEC performance.

2. Experimental

$CdSO_4$, H_2SO_4, and Na_2SeO_3 were obtained from Sinopharm Chemical Reagent Co., Ltd., China. All reagents used were analytical grade and were used directly without any purification.

Metal Ti (0.5 mm thick, 99.7% purity) foils (1.2 cm × 3 cm) were polished mechanically and cleaned with ethanol, acetone and de-ionized water by ultrasonic for 15 min prior to anodization. Then the Ti foils were immersed in a mixed glycerol solution of 0.75% (vol.) NH_4F, 10% (vol.) H_2O and subjected to a constant 30 V anodic potential for 3 h at room temperature in a two-electrode electrochemical cell connected to a DC power supply (LONGWEI Instruments (HK) Co., Ltd. – TPR-12003D), with a graphite flake of about 5.0 cm^2 used as the auxiliary electrode. After anodic oxidation, the samples were rinsed with de-ionized water, and dried in a N_2 stream. The resulting amorphous NTAs were annealed at 600 °C for 2 h in air and cooled naturally.

Electrodeposition of CdSe/TiO_2 NTAs was carried out in a conventional three-electrode cell using a Chi750B electrochemical workstation. The working electrode was TiO_2 NTAs after calcined at 600 °C. A graphite rod of about 4.0 cm^2 and a saturated Ag/AgCl electrode served as the counter and reference electrodes, respectively. Electrodepsition of CdSe/TiO_2 NTAs was carried out in a solution of 0.25 M $CdSO_4$ + 0.25 M H_2SO_4 + 14 mM Na_2SeO_3 at ambient temperature using cyclic voltammetry technique, sweeping the potential between 0 and −1 V at a sweep rate of 0.1 V/s for different number of cycles (marked as "r" in the following figures). After electrodeposition, the samples were thoroughly rinsed with de-ionized water. To get better crystalline of CdSe, the prepared CdSe/TiO_2 electrodes were annealed at 450 °C for 1 h in N_2 stream and cooled to room temperature.

The obtained deposits were characterized by field emission scanning electron microscope (FE-SEM, JSM-6330F), X-ray diffractometer (XRD, D8 ADVANCE) with Cu Kα radiation (λ = 1.5418 Å), transmission electron microscopy (TEM, JEM2010-HR). The optical properties of the CdSe/TiO_2 hybrid NTAs were measured with a UV–vis–NIR Spectrophotometer (UV, Shimadzu UV-3150).

The PEC properties of the TiO_2 NTAs electrodes were measured as follows: the photocurrent (I) and photovoltage (V) of the cell were measured with an active TiO_2 nanotube electrode having an area of 0.60 cm^2 under simulated sunlight which was produced by a 500 W Xenon lamp (PLS-LAX500, Perfectlight, Beijing). A UV filter (absorb $\lambda \leq 420$ nm) was used to cut off the UV energy. An

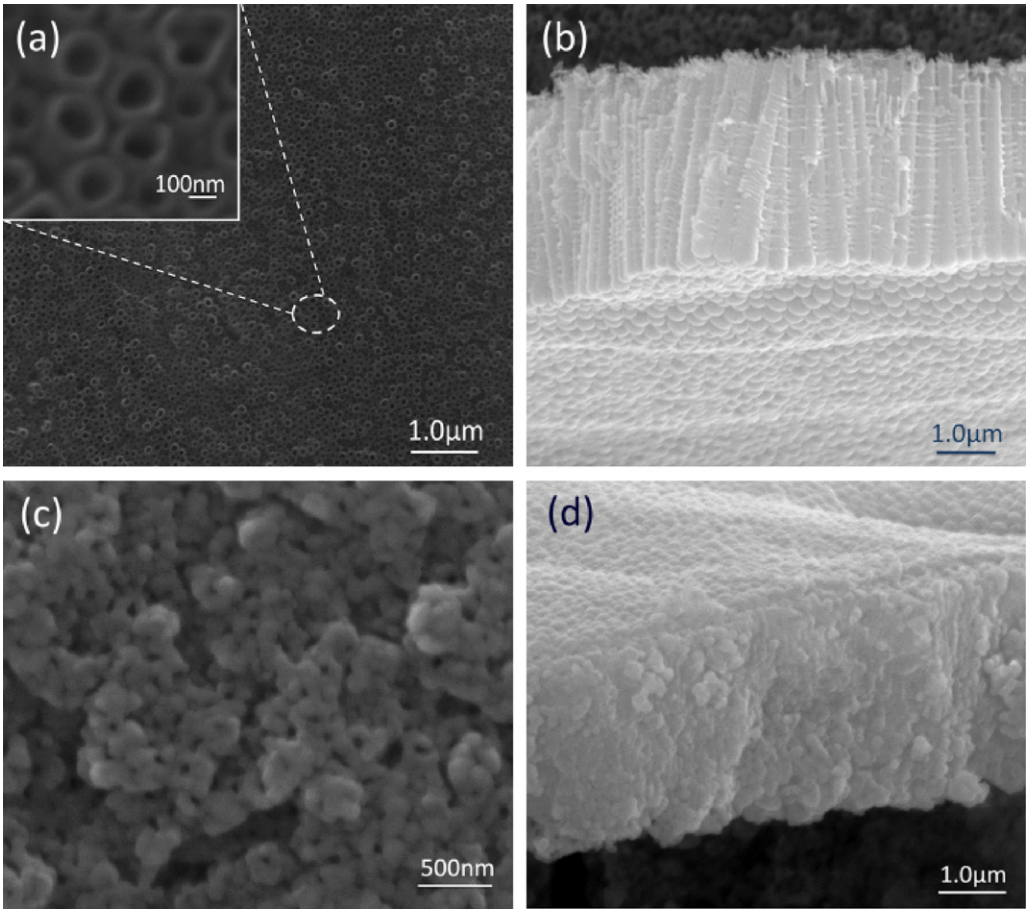

Fig. 1. Morphologies of TiO_2 and CdSe/TiO_2 NTAs film: (a) a typical top view SEM image of the TiO_2 nanotube array film; (b) a cross-sectional view of the well aligned TiO_2 nanotube film. SEM images showing CdSe deposited TiO_2 NTAs film at (c) and (d) cross-sectional view.

electrochemical analyzer (Chi750a electrochemical workstation) was used to measure the PEC response of the samples, with conventional three-electrode system comprising of an Ag/AgCl reference electrode, a graphite rod of about 4.0 cm^2 counter electrode and the sample electrode. All potentials are reported relative to the Ag/AgCl reference electrode. A 0.1 M Na_2S aqueous solution was used as the electrolyte.

3. Results and discussion

The SEM images of as-prepared TiO_2 NTAs are shown in Fig. 1a and b. The nanotubes have an average inner diameter of 100 nm and an interpore distance of 170 nm, as shown in Fig. 1a. TiO_2 NTAs of 2.5 μm in length were obtained after 3 h anodization (Fig. 1b). Fig. 1c shows that the CdSe was well distributed on the top surface of the TiO_2 NTAs. The lateral view in Fig. 1d further confirms that the length of TiO_2 NTs is 2.5 μm and the CdSe was deposited on the outer spaces of the NTAs.

The XRD patterns of as-anodized TiO_2, annealed TiO_2 at 600 °C, and CdSe/TiO_2 NTAs with 30 deposited cycles are shown in Fig. 2. Its evident from Fig. 2a that the as-prepared TiO_2 nanotubes were amorphous. After annealing at 600 °C for 3 h in air, the main peaks for anatase and rutile phase TiO_2 are detected in the pattern b and c (JCPDS 21-1272). The Ti peaks are also observed in XRD, which are according to the Ti substrates. The CdSe deposited belongs to the zinc blende structure with lattice constants a = 6.05 Å (JCPDS 65-2891) (Fig. 2c).

Typical TEM images of CdSe/TiO_2 NTAs are shown in Fig. 3a and b. These nanotubes have uniform size with the average diameters of about 100 nm, which is in agreement with SEM images. The products were further characterized by high resolution transmission electron microscopy (HRTEM). The bright field TEM image of this specimen clearly indicates a porous structure of the TiO_2 matrix (Fig. 3a). When focused around the pore interface, crystalline planes were clearly observed (Fig. 3b). The lattice spacing measured for this crystalline plane is 0.35 nm, corresponding to the (1 0 1) plane of anatase TiO_2. By measuring the lattice parameters and comparing with the data in JCPDS, the crystallites loading on the TiO_2 are CdSe (0.30 nm lattice spacing marked by a dashed ellipse in Fig. 3b), which is according to the results of XRD. Therefore, the HRTEM observation further demonstrates the CdSe assembled on the TiO_2 surface. And the corresponding FFT image inset in Fig. 3b also indicates that the CdSe/TiO_2 composite is presented in a poor polycrystalline structure.

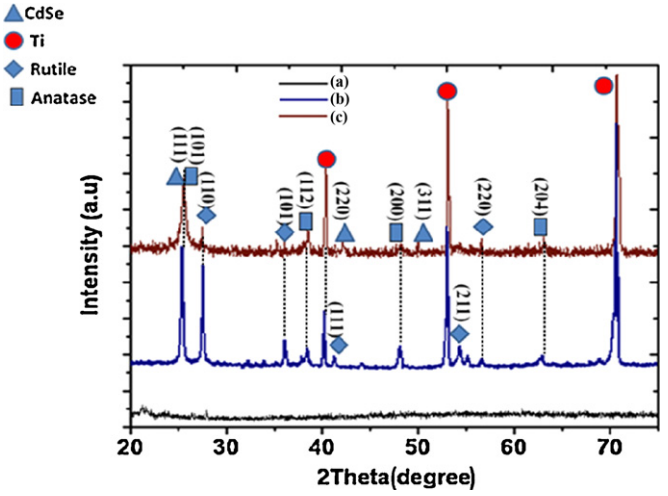

Fig. 2. Experimental XRD profiles taken from (a) amorphous TiO_2 NTAs; (b) TiO_2 thermal annealed at 600 °C; (c) CdSe deposited TiO_2 nanotube film. The peaks are denoted by oblong = TiO_2 anatase, circle = metal titanium substrate, triangle = CdSe, and rhombus = TiO_2 rutile.

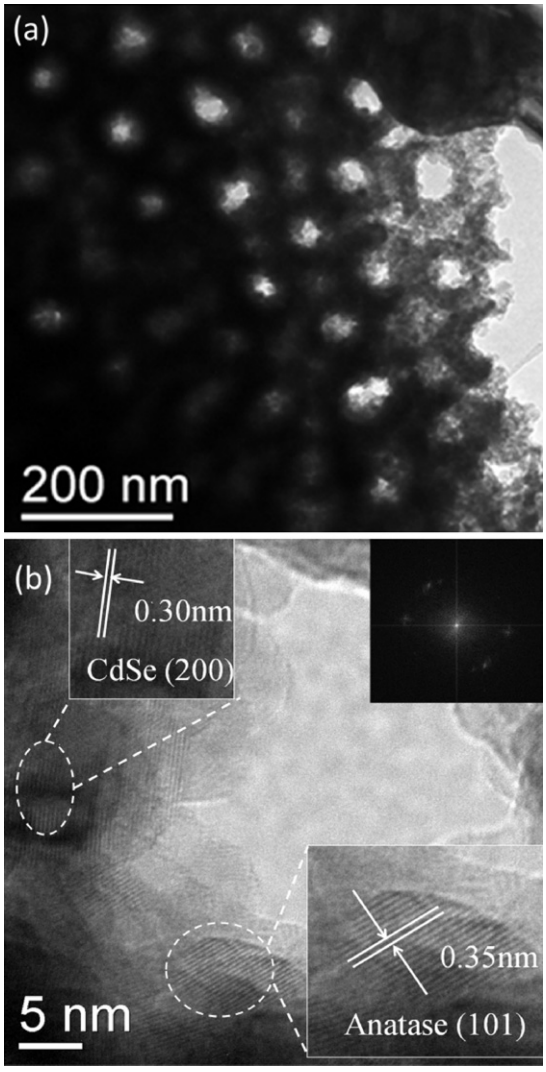

Fig. 3. (a) TEM images of the TiO_2 nanotube film after CdSe were deposited into the film; (b) a HRTEM image and corresponding FFT image inset of a CdSe deposited nanotube.

The absorption spectra of CdSe/TiO_2 NTAs are shown in Fig. 4. The pure TiO_2 NTAs have absorption wavelength below 390 nm, exhibiting a fundamental absorption edge corresponding to the band-gap energy of 3.2 eV in the ultraviolet region. Comparatively, CdSe/TiO_2 NTAs samples show enhanced absorptions in the range from 400 to 750 nm with different amount of CdSe, suggesting they can absorb more visible light to generate more electron–hole pairs. Specifically, the ordered and porous TiO_2 support has interior surfaces on which CdSe nanoparticles can be deposited, resulting in an enhancing absorption capacity in the visible light region while collecting and transmitting electrons through the TiO_2 NT network. This may suggest that the nanocomposite is expected to increase photogenerated charge carriers under the irradiation of visible light. Moreover, the enhancement of crystallinity and the reduction of surface defect sites of CdSe/TiO_2 NTAs via calcination provide an efficient electron transport pathway. As a result, the transport of the photogenerated electrons from CdSe to TiO_2 will be facile and the recombination between the electrons and holes will be restrained.

The current–voltage (I–V) characteristics of pristine TiO_2 and CdSe/TiO_2 electrodes are shown in Fig. 5a. Both the films show

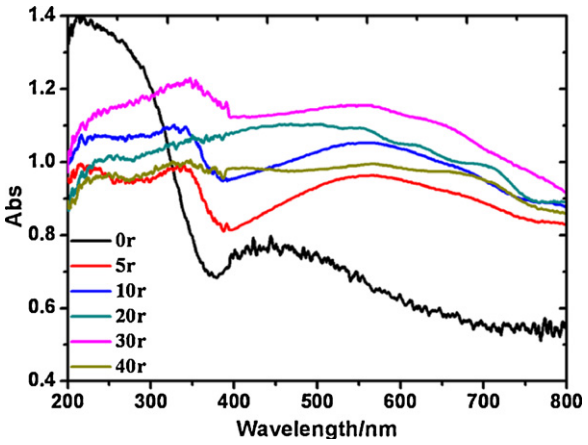

Fig. 4. UV absorption spectrum of the prepared TiO_2 nanotube deposited by different amount of CdSe.

photocurrents when subjected to band gap excitation. It is obvious that the current density of CdSe/TiO_2 is up to 7.1 mA/cm^2, which is 7 times higher than pristine TiO_2 under light illumination. A similar photocurrent response has been reported by spray pyrolysis deposited CdSe/TiO_2 films from aqueous solutions of 0.1 M cadmium chloride and 0.1 M sodium selenosulfate by Shin et al. [32] They found that the photocurrent response of the CdS or CdSe modified 400 nm-length TiO_2 nanotube arrays is 25 times higher than that of the neat 400 nm-length TiO_2 nanotube arrays. When the tube length was 3 μm, the CdSe decorated TiO_2 nanotube arrays showed a photocurrent density of about 10 mA/cm^2, which is higher than our results due to the length of the NTAs are shorter than 3 μm in this research. The observed photocurrents increase as the potential is swept toward positive values. We observe zero current at potentials of −0.86 and −1.10 V vs. Ag/AgCl for TiO_2 and CdSe/TiO_2 electrode, respectively. The 0.24 V shift represents the improved energetics of the CdSe/TiO_2 films and shows the advantage of using composite nanostructures for boosting open circuit potentials. The higher photocurrent density and the more negative zero-current potentials on CdSe/TiO_2 NTs further confirm that 30 cycles deposited CdSe can separate photogenerated pairs more effectively than do the pristine ones.

As is shown in Fig. 5b, the photocurrent collected on the 30 cycles deposited CdSe/TiO_2 NTAs is the highest, which depicts a decrease in the initial excitation period under the illumination. The maximum photocurrent appears to be constant at 1.6 mA/cm^2. And the same decay of photocurrent is also observed on the other CdSe/TiO_2 specimen. Consequently, the fast decay of the photocurrents on CdSe/TiO_2 NTs in the initial excitation period under intense light illumination in PEC detection can be attributed to these reasons listed below: (i) fast recombination between photogenerated holes and electrons resulting from the abundant generated carriers in the initial several seconds (the hole-scavenger had difficulty in depleting so many holes in such a short time due to the mass transport limitations) and (ii) large CdSe particles that accumulate dozens of electrons, may serve as the recombination centers of the photogenerated holes and electrons and cannot inject electrons into the TiO_2 NT network as effectively as smaller amount of CdSe nanoparticles [33]. In the present study, the second reason can explain the generation of the high photocurrent obtained on 30 cycles deposited CdSe/TiO_2 NTAs, instead of that obtained on 40 cycles. The 5 cycles deposited CdSe/TiO_2 NTAs did not exhibit a high photocurrent, which may be attributed to the low CdSe loading contents, resulting in a less absorption of visible light. Compared with the similar results of Kongkanand et al. [33] the maximum photocurrent response was seen to be 2.4 mA/cm^2 by 3.0 nm-CdSe/TiO_2 electrodes, while 1.7 mA/cm^2 was observed from 3.7 nm-CdSe/

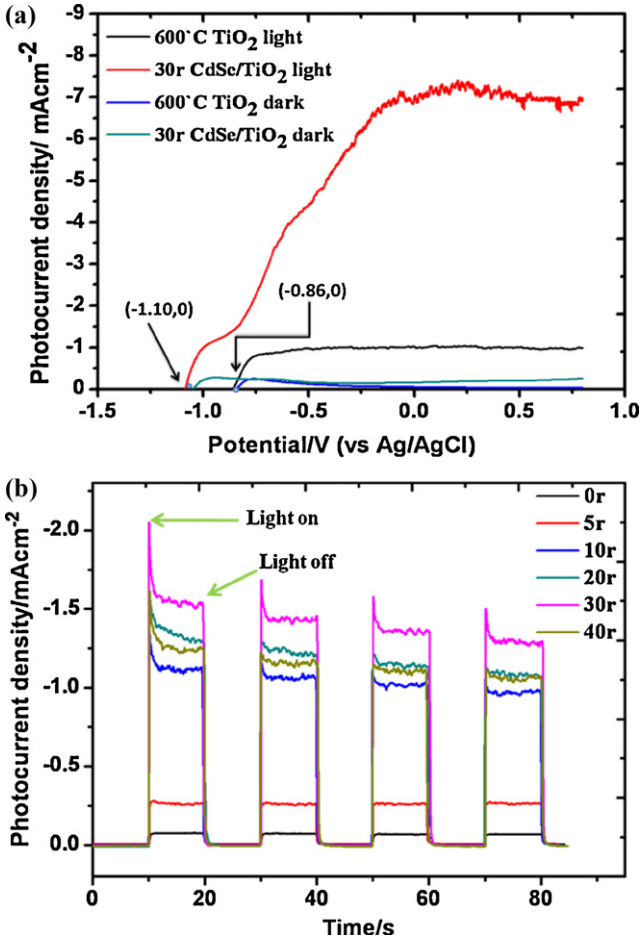

Fig. 5. (a) The current–voltage (I–V curve) characteristics of TiO_2 nanotube and TiO_2 nanotube deposited by 30cycles of CdSe in 0.1 M Na_2S; (b) photocurrent intensity (i–t curve) of TiO_2 nanotube deposited by different amount of CdSe in 0.1 M Na_2S.

TiO_2. Our results well match the reason that, decreasing particle size of CdSe in a certain range increases photocurrent as the shift in the conduction band to more-negative potentials increases the driving force for charge injection.

The strong photoresponse (Fig. 5a) and enhanced photostability (Fig. 5b) are attributed to three major improvements. Firstly, during the electrodeposition process, TiO_2 nanotubes are filled with a host of CdSe particles with small diameter, and uniform distribution. Secondly, increased light absorbability and better light scattering are produced within the CdSe/TiO_2 NTAs structure. Additionally, the photo-generated charge carriers in the CdSe/TiO_2 nanotubular structure are separated more efficiently than in the pure TiO_2 nanotube structure due to the favorable electron and hole transfer as mention before. The basic structure of the CdSe/TiO_2 NTAs electrode is presented in Fig. 6 and the main charge-transfer processes between TiO_2 and CdSe after being activated by the light. The coupling of the semiconductors has a beneficial role in improving charge separation. Excited electrons from the CdSe can quickly transfer to the TiO_2 nanotube, arriving at the photocurrent collector (Ti substrate) through the highly ordered TiO_2 nanotube array structure with well crystalline nature. The responsive photocurrent intensity is usually able to directly represent the overall photoelectron-conversion process. One is note that the crystalline structure has a great influence on the PEC performance of CdSe/TiO_2 nanotube arrays. Chiarello et al. [34] found that different crystal phase and surface area are key factors influencing the photoactivity. For example, home-made photocatalyst mainly consisting of rutile and also containing a brookite fraction is a very good photocatalyst for

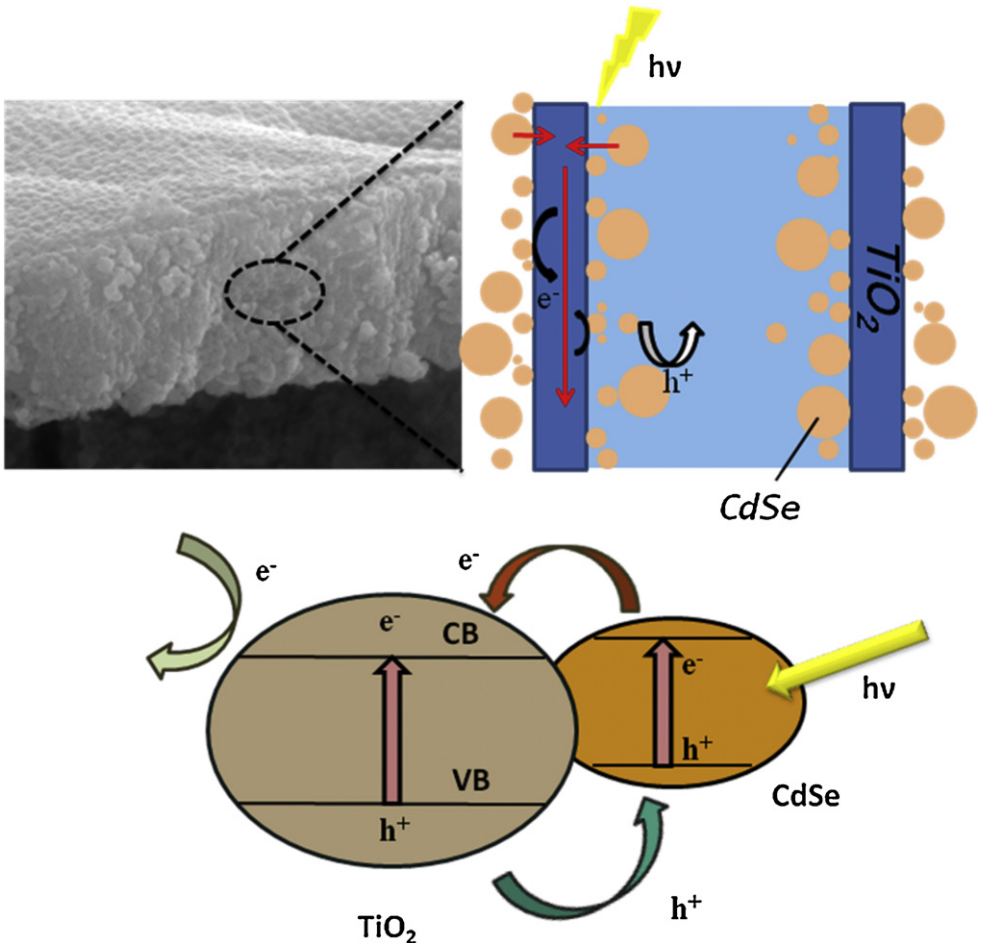

Fig. 6. The main charge-transfer process between TiO_2 and CdSe after being excited by light. (CB and VB refer to the energy levels of the conduction and valence bands, respectively, for the CdSe and TiO_2 nanotube.

hydrogen production under UV–vis irradiation, whereas commercial rutile is less photoactive TiO_2 polymorph.

4. Conclusion

In summary, we demonstrated a simple and environmental electrochemical approach to synthesize CdSe/TiO_2 NTAs which extends significantly the photoresponse of the TiO_2 NTAs into the visible region and improves its photoactivity and photostability. In the coupled semiconductor system, the small band-gap semiconductor CdSe acts as a photosensitizer for the TiO_2. Our results show that smaller-amount CdSe/TiO_2 possess greater charge injection rates. Larger-CdSe-amount has better absorption in the visible region but cannot inject electrons into TiO_2 as effectively as smaller-amount CdSe, due to the interplay of various factors. The significant photocurrent achieved here also proves that the unique nanotube structures can facilitate the propagation and kinetic separation of photogenerated charges. Furthermore, the application of the electrodeposition technique shows good control over CdSe/TiO_2 nanostructures, leading to better solar light harvest in the visible light region of this class of materials. Thus, this method provides a promising technique to fabricate excellent composite materials at room temperature, showing potential applications in PEC cells.

Acknowledgments

This work was supported by the Natural Science Foundations of China (Grant No. 90923008 and J1103305), the Natural Science Foundations of Guangdong Province (Grant No. 925102 7501000002), the Academic New Artist Ministry of Education Doctoral Post Graduate, and the Fundamental Research Funds for the Central Universities (101gzd13).

References

[1] H. Kato, K. Asakura, A. Kudo, J. Am. Ceram. Soc. 125 (2003) 3082.
[2] Y. Wang, Z. Zhang, Y. Zhu, Z. Li, R. Vajtai, L. Ci, P.M. Ajayan, ACS Nano 2 (2008) 1492.
[3] J. Li, J. Wang, L. Huang, G. Lu, Photochem. Photobiol. Sci 9 (2010) 39.
[4] M. Gratzel, Nature 414 (2001) 338.
[5] K. Honda, A. Fujishima, Nature 238 (1972) 37.
[6] S.U.M. Khan, W.B.I. M. Al-Shahry Jr., Science 297 (2002) 2243.
[7] Z. Liu, Y. Li, Z. Zhao, Y. Cui, K. Hara, J. Mater. Chem. 20 (2010) 492.
[8] W. Choi, A. Termin, M.R. Hoffmann, J. Phys. Chem. 98 (1994) 13669.
[9] A. Hagfeldt, M. Gratzel, Chem. Rev. 95 (1995) 49.
[10] R. Asahi, T. Morikawa, T. Ohwaki, K. Aoki, Y. Taga, Science 293 (2001) 269.
[11] J.H. Park, S. Kim, A.J. Bard, Nano Lett. 6 (2006) 24.
[12] K. Rajeshwar, J. Appl. Electrochem. 37 (2007) 765.
[13] C. Burda, Y. Lou, X. Chen, A.C.S. Samia, J. Stout, J.L. Gole, Nano Lett. 3 (2003) 1049.
[14] S. Pavasupree, J. Jitputti, S. Ngamsinlapasathian, S. Yoshikawa, Mater. Res. Bull. 43 (2008) 149.
[15] F. Sayılkan, M. Asiltürk, P. Tatar, N. Kiraz, S. Sener, E. Arpac, H. Sayılkan, Mater. Res. Bull. 43 (2008) 127.
[16] R. Vogel, P. Hoyer, H. Weller, J. Phys. Chem. 98 (1994) 3183.
[17] C.B. Murray, D.J. Norris, M.G. Bawendi, J. Am. Ceram. Soc. 115 (1993) 8706.
[18] T. Lo'pez, F. Rojas, R. Alexander-Katz, F. Galindo, A. Balankin, A. Buljan, J. Solid State Chem. 177 (2004) 1873.
[19] R. Plass, S. Pelet, J. Krueger, M. Gratzel, J. Phys. Chem. B 106 (2002) 7578.
[20] S.C. Lin, Y.L. Lee, C.H. Chang, Y.J. Shen, Y.M. Yang, Appl. Phys. Lett. 90 (2007) 143517.
[21] W.T. Sun, Y. Yu, H.Y. Pan, X.F. Gao, Q. Chen, L.M. Peng, J. Am. Ceram. Soc. 130 (2008) 1124.
[22] C. Karunakaran, G. Abiramasundari, P. Gomathisankar, G. Manikandan, V. Anandi, Mater. Res. Bull. 46 (2011) 1586.

[23] I. Robel, V. Subramanian, M. Kuno, P.V. Kamat, J. Am. Ceram. Soc. 128 (2006) 2385.
[24] Y.H. Xu, D.H. Liang, M.L. Liu, D.Z. Liu, Mater. Res. Bull. 43 (2008) 3474.
[25] D. Falcomer, M. Daldosso, C. Cannas, A. Musinu, B. Lasio, S. Enzo, A. Speghini, M. Bettinelli, J. Solid State Chem. 179 (2006) 2452.
[26] L.M. Peter, K.G.U. Wijayantha, D.J. Riley, J.P. Waggett, J. Phys. Chem. B 107 (2003) 8378.
[27] P. Kar, K.S. Raja, M. Misra, B.N. Agasanapur, Mater. Res. Bull. 44 (2009) 398.
[28] K. Zhu, N.R. Neale, A. Miedaner, A.J. Frank, Nano Lett. 7 (2007) 69.
[29] H. Cao, Y. Zhu, X. Tan, H. Kang, X. Yang, C. Li, New J. Chem. 34 (2010) 1116.
[30] G.W. She, X.H. Zhang, W.S. Shi, X. Fan, J.C. Chang, C.S. Lee, S.T. Lee, C.H. Liu, Appl. Phys. Lett. 92 (2008) 05311.
[31] D. Pradhan, K.T. Leung, Langmuir 24 (2008) 9707.
[32] K. Shin, S. Seok, S.H. Im, J.H. Park, Chem. Commun. 46 (2010) 2385.
[33] A. Kongkanand, K. Tvrdy, K. Takechi, M. Kuno, P.V. Kamat, J. Am. Ceram. Soc. 130 (2008) 4007.
[34] G.L. Chiarello, A.D. Paola, L. Palmisano, E. Selli, Photochem. Photobiol. Sci 10 (2011) 355.